PROCEEDINGS, 43rd Workshop on Geothermal Reservoir Engineering
Stanford University, Stanford, California, February 12-14, 2018
SGP-TR-213

Temperature-Dependent Kinetics of Phenyl Acetate Hydrolysis

Xiang Gu[1,2], Adam J. Hawkins[2,3,4], and Jefferson W. Tester[1,2]

[1]Cornell University, Robert Frederick Smith School of Chemical and Bimolecular Engineering, Ithaca, NY 14853

[2]Cornell University, Cornell Energy Institute, Ithaca, NY 14853

[3]Stanford University, TomKat Center for Sustainable Energy, Stanford, CA 94305

[4]Stanford University, Energy Resources Engineering, Stanford, CA 94305

xg248@cornell.edu

Keywords: thermally reactive tracers, base-catalyzed hydrolysis, reaction kinetics, temperature dependency, effects of mineral surface.

ABSTRACT

In field work evaluation of using phenyl acetate as a thermally degrading tracer, we discovered that its hydrolysis is catalyzed by a heterogeneous reaction in the presence of silica surfaces. The catalytic effect of crushed sandstone, the host reservoir mineral in our field tests, was measured in a well-controlled fluid system over a range of fluid and mineral conditions. Under homogeneous conditions without minerals present, phenyl acetate hydrolysis is first-order and base-catalyzed at a pH of roughly 6.3 for temperatures from 10 to 65 °C. Arrhenius parameters under homogeneous conditions were consistent with previous investigations. In a mixture of 100 ml of reacting fluid with 0.2-2 g crushed sandstone having a nominal particle diameter of 100 μm, the reaction rate increased dramatically. However, the catalytic effect develops slowly. In fact, a very limited catalytic effect is observed if mineral surfaces are only in contact with aqueous solution for short periods prior to introducing phenyl acetate. For longer exposure times catalytic effect can be significant, e.g. at 70 days, reaction rates doubled. Multiple techniques including SEM were employed to characterize the surface of the crushed sandstone particles.

1. INTRODUCTION

Geothermal energy is playing an increasingly important role in meeting the growing demand for sustainable renewable energy. To utilize geothermal energy in an effective and efficient fashion, it is crucial to estimate the thermal lifetime of geothermal reservoirs and to anticipate early thermal breakthrough if it occurs during production. A sudden decline in production temperature without warning could lead to a series of economic and environmental issues. Being able to quantitatively characterize the progress of thermal drawdown within a geothermal reservoir can indicate if the given geothermal system is operating at, or near, an ideal production rate.

Reinjection of produced fluids after a portion of their thermal energy is consumed is a commonly-employed strategy to maintain reservoir pressures and production rates and to decrease any negative environmental impacts caused by discharging reservoir fluids (Horne, 1985). Unfortunately, for many geothermal power plants that use reinjection, early temperature decline often occurs due to unanticipated short circuiting of fluid within the reservoir between the injection and production wells. Diaz et al. (2016) has documented the negative impacts of reinjection on commercial geothermal reservoirs in a recent review paper. For example, early thermal breakthrough has been observed in geothermal fields at Ahuachapán, in El Salvador (Vides-Ramos, 1985), Palinpinon, in the Philippines (Malate and O'Sullivan, 1991), and Svartsengi, in Iceland (Björnsson and Steingrimsson, 1992). Therefore, the geothermal industry would benefit from diagnostic tools capable of monitoring the spatial and temporal behavior of reservoir temperatures. During production, the geothermal reservoir cools gradually starting at the injection point and the induced cold front migrates towards the production wells. However, the rate of migration and eventual temperature breakthrough at the production well is challenging to monitor directly due to the high cost of drilling a sufficient number of monitoring wells. Computational modeling can provide predictions of thermal breakthrough, however, sufficient calibration of these models is rarely achieved due to the complexity of fluid flow path distribution between injectors and producers.

A common approach to calibrate such models is to measure subsurface Residence Time Distributions (RTDs) and effective fluid volumes within the reservoir using an inert (i.e., conservative) tracer. However, it is the effective heat transfer area that dominates thermal breakthrough (Hawkins et al., 2017a, 2017b). Thermally degrading tracers were proposed several decades ago to overcome the limitations of inert tracers by providing a convenient means to estimate reservoir thermal drawdown in-situ (Robinson et al., 1988). Using the Arrhenius Law, the temperature dependency of reactive tracers can be determined quantitatively and investigated as an *in-situ* measurement of subsurface reservoir temperature. Despite the encouraging initial laboratory work, further attempts to test these thermally degrading tracers have seen only limited success. In Hawkins et al. (2017a) summarizes field tests involving thermally degrading tracers and the first use of phenyl acetate in field experiments is presented. Field testing confirmed, qualitatively, that phenyl acetate can track the progression of a thermal front between two wells. However, phenyl acetate did not experience reaction rates consistent with laboratory batch reactor measurements presented in Nottebohm et al. (2012) or in column tests presented in Maier et al. (2015). As a result, quantitative estimates of inter-well fluid temperatures were inaccurate and the reaction rates observed in the field were more than 7000x greater than reported in Nottebohm et al. (2012).

2. OBJECTIVES AND APPROACH

This study aims to improve the understanding of phenyl acetate hydrolysis kinetics and the interpretation of tracer data on a laboratory scale. First, homogenous hydrolysis measurements using batch reactor experiments presented by Nottebohm et al. (2012) were repeated in our laboratory. Second, heterogeneous reactions in the presence of mineral particles were investigated. Reaction rates were measured at fixed temperatures and pH values in the presence of varying fluid/mineral surface areas.

The specific objectives of this study were to:

1) Determine appropriate assumptions for phenyl acetate hydrolysis process;

2) Investigate the temperature dependency and concentration dependency of the reactive tracer in homogeneous and heterogeneous systems.

The experimental approach used in our laboratory work to determine the hydrolysis reaction kinetics of phenyl acetate includes:

1) Measure the tracer concentration as a function of time and calculate the corresponding reaction rate constants under various controlled reaction conditions (temperature, pH, pretreatment time, and total reactive area of rock particle surfaces);

2) Plot Arrhenius diagrams to illustrate the temperature dependency of tracer reactions under varying conditions;

3) Using SEM, characterize surfaces of the given rock particles.

3. METHODS

3.1 Field Site

The Altona field site used in this study is located in northern New York, USA. The site was selected because it has relatively shallow water levels and a highly permeable sub-horizontal bedding plane fracture at 7.6 m below ground surface (Hawkins et al., 2017a). Since 2004, this field site has been utilized in numerous investigations of heat and mass transport in a heterogeneous fracture (e.g., Becker et al., 2013; Becker and Tsoflias, 2010; Hawkins, 2013; Hawkins, 2017; Hawkins et al., 2017a; Hawkins et al., 2017b; Hawkins et al., 2018; etc.). The relevant geologic formation at Altona is the Potsdam Sandstone, which, locally, has very low matrix porosity (<3%) and extensive bedding plane fracturing.

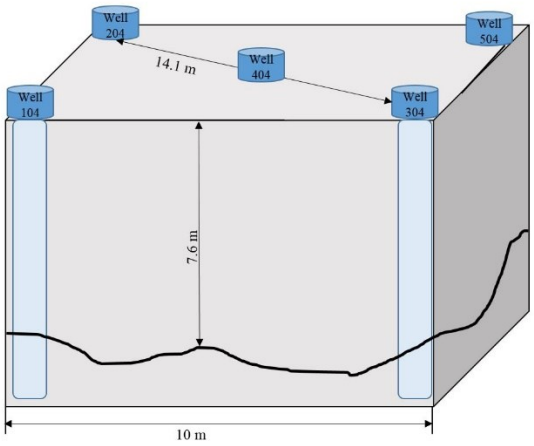

Figure 1: Three-dimensional schematic of the Altona field testing in which the working fluid was continuously circulated between the injection well 204 and the production well 304. Observation wells (104, 404, and 504) are indicated on the schematic as well.

To investigate the apparent catalytic effect of the Potsdam sandstone on phenyl acetate hydrolysis, samples of the Potsdam were collected from drill cuttings (Fig. 2). Drilling activities were conducted in 2011 and cuttings were collected at a depth of roughly 9.1 m below ground surface. Average particle diameter is estimated to be roughly 100 μm based on SEM imaging (Fig. 2). Assuming particles are roughly spherical, the average nominal particle surface area and volume are 3.14×10^{-4} cm^2 and 5.23×10^{-7} cm^3, respectively. Potsdam sandstone has a density of 2.5 g/cm^3 (Hawkins, 2017), which results in a surface area per unit mass ratio of roughly 240 cm^2/g.

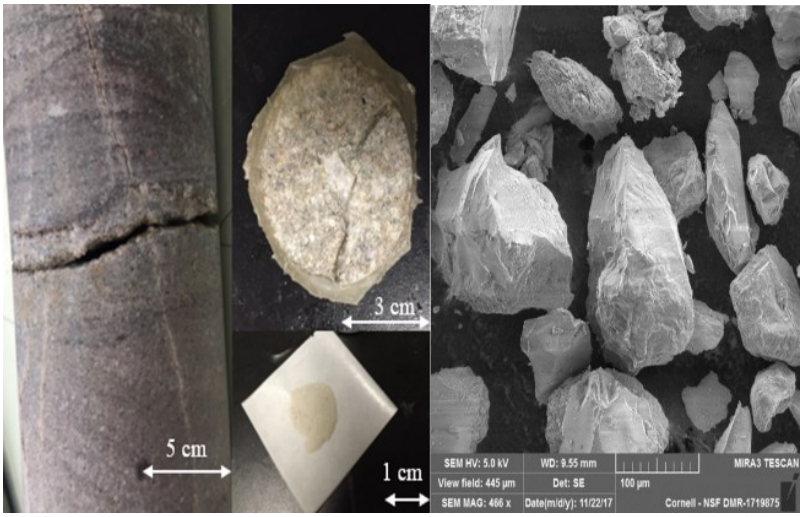

Figure 2: Photograph of the crushed Potsdam Sandstone collected from the Altona field site (left) and a SEM image of the crushed Potsdam Sandstone (right).

3.2 Hydrolysis of Phenyl Acetate

Phenyl acetate hydrolyzes rapidly at low-temperature and was therefore appropriate for the low-temperature conditions at the Altona field site (Nottebohm et al., 2012). In a given geothermal system, the transport and reaction of phenyl acetate occurs simultaneously. Although flow in a discretely fractured reservoir is essentially two–dimensional, we can simply the reservoir by assuming that fluids are transported through a streamtube in one-dimension with the overall transport phenomenon described as follows:

$$\frac{\partial c}{\partial t} = D_f \frac{\partial^2 c}{\partial t^2} - v \frac{\partial c}{\partial t} - kc \tag{1}$$

where *c, t,* D_f*, v, kc* are tracer fluid concentration in the fracture [M/L^3], time, the one-dimensional hydrodynamic dispersion coefficient [L^2/t], the average fluid velocity across the fracture aperture [L/t], and the reaction rate constant [1/t], respectively. The last term *(kc)* on the right-hand side of this equation describes the influence of the reaction rate on the transport of tracer, and is the most relevant parameter in this study.

Schwarzenbach and Gschwend (1993) compared the relative importance of the acid versus base-catalyzed hydrolysis for some common carboxylic acid esters. They found that esters with good leaving groups and/or electron-withdrawing substituents in the acid part of the molecule are more likely to undergo base-catalyzed hydrolysis in near-neutral systems, including phenyl acetate. Even though hydrolysis is pH-dependent, generally speaking geothermal systems are not likely to have large variations in pH (Nottebohm, 2012). Therefore for those cases, reaction rates can correctly be characterized by the reaction rate at an average pH. At the Altona field site, measured fracture fluids are near-neutral with a pH of 6.5. Therefore, phenyl acetate hydrolysis at conditions appropriate for the Altona field site is assumed to be base-catalyzed with an over mechanism depicted in Fig. 3. See Nottebohm et al. (2012) for further description of the hydrolysis reaction. Schwarzenbach and Gschwend (1993) pointed out that for esters exhibiting an aromatic alcohol moiety (e.g., for phenyl esters), the formation of the tetrahedral intermediate is rate limiting as shown in Eqn. (2). They also mentioned that in Eqn. (3), the breakdown of the tetrahedral intermediate may be kinetically important. According to their work, the derived rate law in terms of starting compounds is shown in Eqn. (5) with three rate constants k_{B1}, k_{B2}, and k_{B3}. Note that k_{B4} is not shown in Eqn. (5) since its reactants, acetate and the tetrahedral intermediate, are removed very quickly by deprotonation and protonation, respectively. Since determining these individual rate constants is not realistic in this study, a global reaction rate constant, k_{global}, was used (Eqn. (6)) and was calculated based on our laboratory batch reactor experiments. Equation (6) indicates that the pH value of the system strongly influences the reaction rate constant and that the reaction is linearly correlated with the concentration of hydroxide ions.

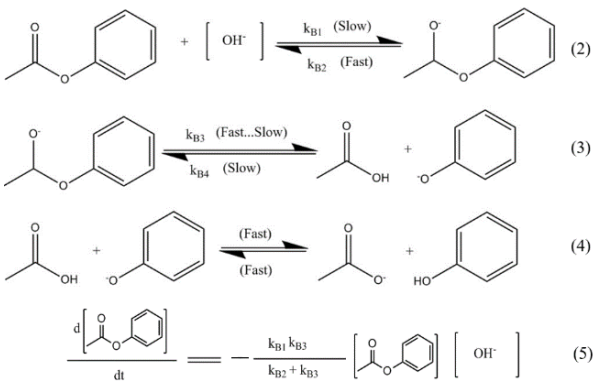

Figure 3: Overall Reaction scheme for the base-catalyzed hydrolysis of phenyl acetate. Phenyl acetate undergoes the hydrolysis to form phenol and acetate.

$$k_{global} = \frac{k_{B1}k_{B3}}{k_{B2} + k_{B3}} \cdot [OH^-] \tag{6}$$

Assuming the temperature-dependency following the Arrhenius Law, k_{global} is

$$k_{global} = A \cdot \exp\left(-\frac{E_a}{RT}\right), \tag{7}$$

where A, E_a, R, and T are the pre-exponential factor [h^{-1}], activation energy [kJ/mol], the universal gas constant [J/mol/K], and the absolute temperature [K], respectively. With k_{global} and $[OH^-]$ specified in Eqn. (5), the hydrolysis reaction can be regarded as pseudo-first-order. With this simplification, its temperature dependency is determined explicitly using Arrhenius plots of natural log rate versus T^{-1}, as presented in the Results section.

3.3 Temperature Dependency: Rate Law and Arrhenius Equation

According to the rate law, for first-ordered reactions, reaction rate constants can be calculated if the initial concentration, c_0 and the concentration as a function of time, $c(t)$, are known, where

$$\ln \frac{c(t)}{c_0} = -k_{gIobal} \cdot t_i \tag{8}$$

By plotting the linear correlation between the natural log of normalized concentration and the reaction time, the reaction rate constant is equivalent to the slope of the best-fit line through the measured points on the plot.

An Arrhenius plot relates the reaction rate constant, k_{global}, to inverse temperature, T^{-1}, such that

$$\ln k_{global} = -\frac{E_a}{R} \cdot \frac{1}{T} + \ln A. \tag{9}$$

After determining a best-fit linear correlation between measured reaction rate and inverse temperature, the line's slope and y-intercept provide estimates of E_a/R and ln A, respectively. Thus, for any thermally degrading tracer applied in a given geothermal system with known Arrhenius parameters and a measured effective reaction rate constant, an effective average reservoir temperature, T_{eff}, can be estimated by Eqn. (10) (Hawkins et al., 2017a).

$$T_{eff} = -\frac{E_a}{R} \cdot \ln\left(\frac{k_{global}}{A}\right)^{-1} \tag{10}$$

3.4 Experimental Apparatus

Phenyl acetate concentration was measured as a function of time using a continuous flow-through system that circulated traced fluids between a temperature-controlled reaction chamber and a Cary Eclipse Fluorescence Spectrophotometer from Agilent Technologies equipped with a flow-through cuvette (Fig. 4a). Temperature in the reaction chamber was controlled by a water bath (Thermo-Scientific, model no. NESLAB RTE 10) (Fig. 4c). In the reaction chamber (Fig. 4d), 100 ml of fluid contained a sodium citrate buffer solution to control fluid pH throughout each experiment. To initiate the experiment, phenyl acetate was injected into the reactor, resulting in an overall mixed phenyl acetate concentration of 3 ppm. The solution was circulated between the reaction chamber and the fluorescence spectrophotometer via a delivery pump (Master Flex, model no. 752-035) (Fig. 4b).

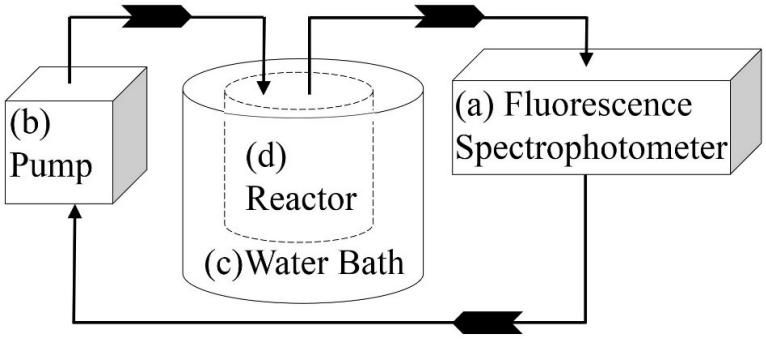

Figure 4: Schematic of the experimental apparatus including (a) A Cary Eclipse Fluorescence Spectrophotometer from Agilent Technologies equipped with a flow-through cuvette; (b) A deliver pump from Master Flex (Model no. 752-035); (c) A water bath from Thermo-Scientific (Model no. NESLAB RTE 10); and (d) A reaction chamber equipped with a pH probe and a propeller.

Concentration of phenol, the reaction product, was measured once per minute continuously throughout each experiment. Assuming mass balance, the concentration of the reaction reactant, phenyl acetate, was determined from the measurement of phenol. A propeller and a pH meter probe were placed in the reaction chamber to keep particles in suspension and to monitor pH continuously. Experiments were conducted at pH range from 6.2 to 6.5 and at temperatures ranging from 10 to 65 ℃. For the heterogeneous experiments, crushed sandstone mass varied from 0.2 to 2 g. An inline 25 μm filter prevented suspended particles from being pumped out of the reaction chamber.

Preliminary experiments showed that the reaction rates vary strongly with the magnitude of contact time between dry rock particles and fluid. Therefore, rock particles were exposed to the aqueous buffer solution for varying timespans before introducing phenyl acetate into the solution. The length of this pretreatment, or "exposure time" $t_{exposure}$, varied from 0 to 120 days.

4. RESULTS AND DISCUSSIONS

4.1 Homogeneous Batch Reactor Experiments

Reaction rates for the homogeneous system were measured at seven different temperatures (10, 20, 30, 40, 50, 60 and 65 ℃) while pH ranged slightly from 6.2 to 6.5 with an effective value of 6.3. The reaction rates ranged from 1.1e-4 h^{-1} (10 ℃) to 0.1470 h^{-1} (60 ℃) (Fig.5). Using Eqn. (9), the Arrhenius parameters for the homogeneous reaction at a pH of 6.3 are 22.1 h^{-1} and 71.4 kJ/mol for ln A and E_a, respectively. In Nottebohm et al. (2012), the Arrhenius parameters were determined for fluids at a pH of both 6 and 7. E_a was 78.0 and 77.0 kJ/mol and ln A was 22.9 and 23.7 h^{-1} for pH of 6 and 7, respectively (Tbl. 1).

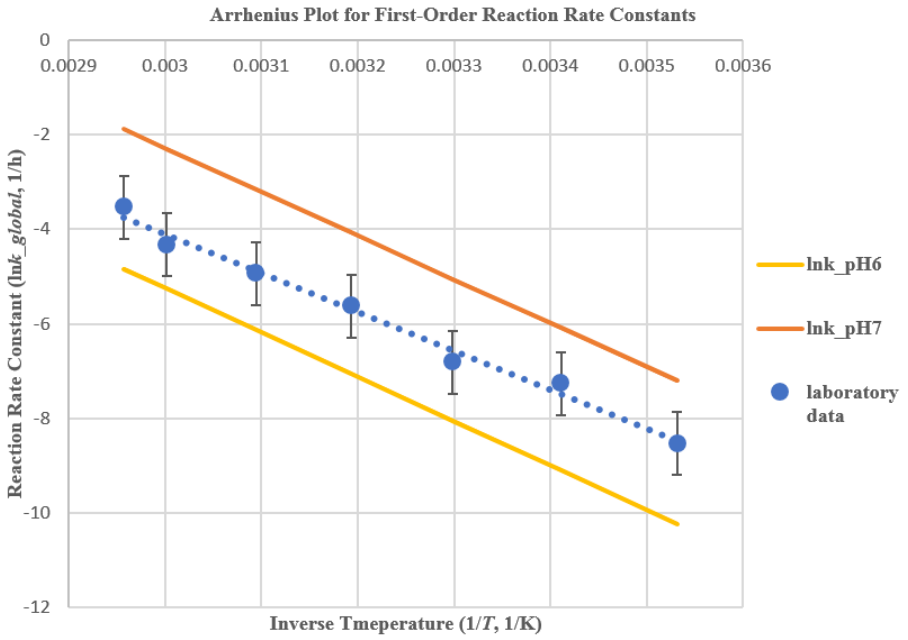

Figure 5: Reaction rate as a function of inverse temperature. Data collected in this study are represented by blue circles and the trend line is plotted as a blue dotted line with 95% confidence intervals. The orange and yellow lines represent the best-fit lines presented in Nottebohm et al (2012).

Table 1: Summary of Arrhenius Parameters

Source	Nottebohm et al., 2012	This study	Nottebohm et al., 2012
pH	6.0	6.3	7.0
E_a(kJ/mol)	78.0	71.4	77.0
$\ln A$ (h^{-1})	22.9	22.1	25.5

4.2 Heterogeneous Batch Reactor Experiments

The reaction rate in the presence of silica surfaces was measured at a fixed pH of 6.3 at temperatures ranging from 18 to 60 °C and with crushed rock masses ranging from 0.2 to 2.0 g. Assuming a surface area per unit mass ratio of roughly 240 cm^2/g (see Section 3.1), this range of mass results in a total surface area ranging from 48.0 to 480.0 cm^2 (Tbl. 2).

Table 2: Crushed rock mass used for each of the four experiments

Experiment Number	1	2	3	4
Total Surface Area (cm^2)	48.0	120.0	240.0	480.0
Crushed Rock Mass (g)	0.2	0.5	1.0	2.0
Activation Energy (E_a, kJ/mol)	65.6	67.1	66.0	70.3
Pre-exponential Factor (ln A, h^{-1})	22.3	23.5	23.6	25.7

The tracer testing at the lowest temperature (18 ℃) was conducted in the presence of 2g rock (480.0 cm^2), the reaction rate constant increased from 0.0007 to 0.0387h^{-1}. At the highest temperature (60 ℃), the experiment was conducted for 1.0 g rock mass, and the reaction rate constant was 0.5734h^{-1}. E_a for the four different experiments ranged from 65.6 to 70.3 kJ/mol and ln A ranged from 22.3 to 25.7 h^{-1}.

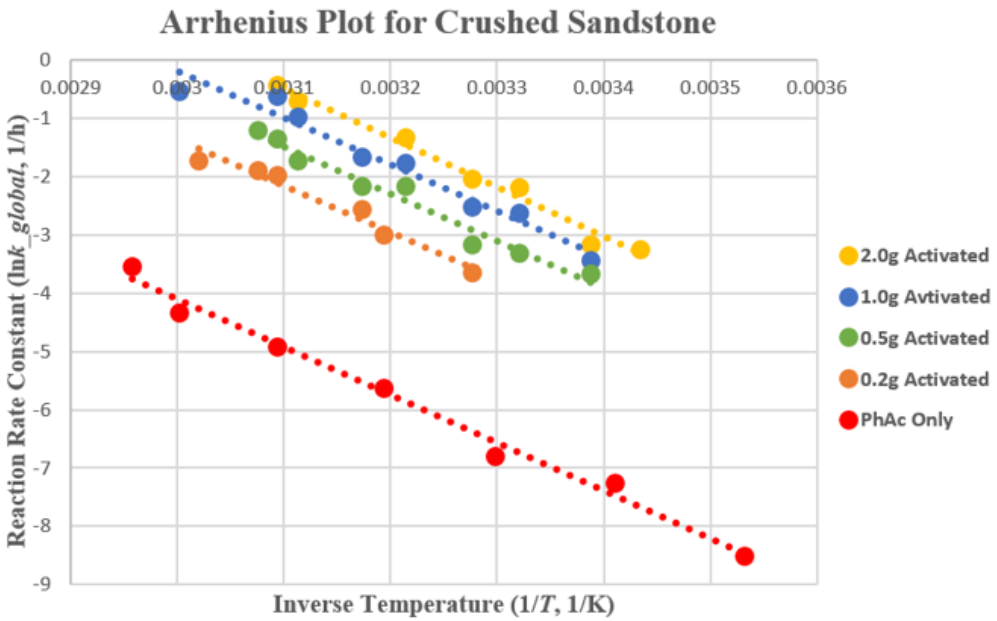

Figure 6: Arrhenius plot for five experiments with varying masses of rock particles. Reaction rate as a function of inverse temperature for the four crushed rock experiments. The homogeneous system ("PhAc Only") is plotted for reference and is identical to the plot in Fig. 5.

As discussed in Section 3.4, preliminary laboratory experiments indicated that the exposure time between crushed rock particles and fluids influences the catalytic effect of the silica surface. The pretreatment time necessary to fully activate the catalytic effect was determined for 1 g of rock by measuring the phenyl acetate hydrolysis reaction rate for a pretreatment time ranging from 0 to 120 days. At 40 °C and a pH of roughly 6.3, 0 days of pretreatment time resulted in a reaction rate constant of 0.1032h^{-1}. The reaction rate rose exponentially as a function of time until it reached 0.2892 h^{-1} at 70 days (Fig. 7). From 70 days to 120 days, the reaction rate remained

relatively constant between 0.2892 and 0.3045 h^{-1}. The correlation between the global reaction rate constant k_{global} and the exposure time $t_{exposure}$ can be described as a piecewise function. From 0 to 70 days, a sufficient fit to measured data was achieved using a polynomial function, where

$$k_{global} = 3*10^{-5} t_{exposure}^2 + 6*10^{-5} t_{exposure} + 0.1095 . \quad (11)$$

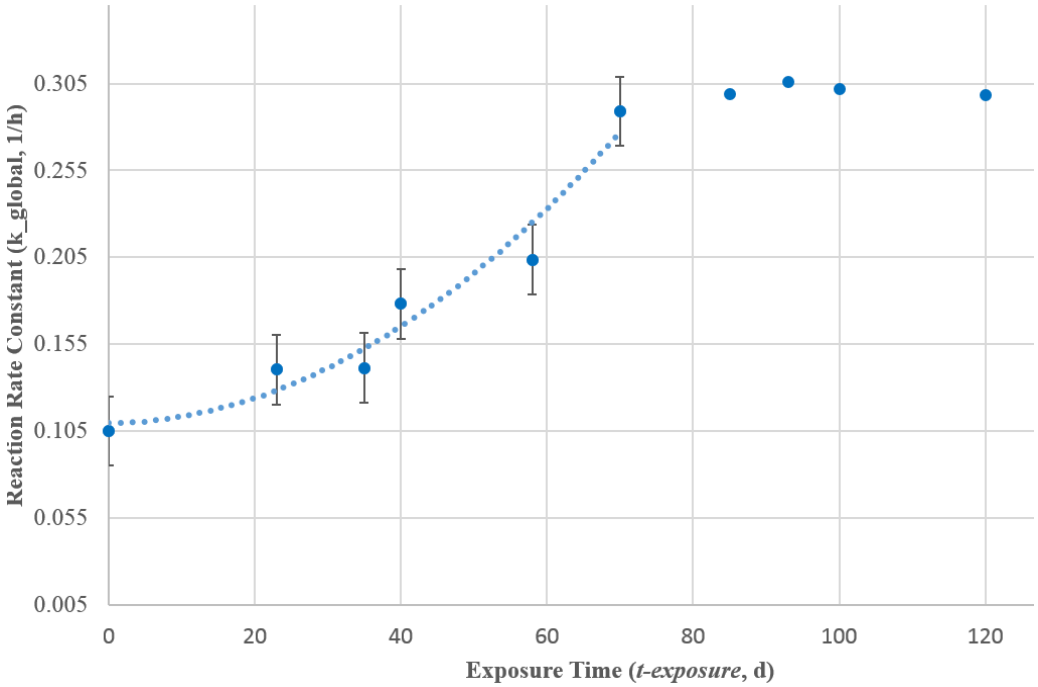

Figure 7: Reaction rate as a function of exposure time between dry particles and fluids at a temperature of 40 °C. The dashed blue line represents the empirical model shown in Eqn. (11). After 70 days, the reaction rate varies little with additional exposure time. The trend line is plotted as a blue dotted line with 95% confidence.

The effect of pretreatment exposure time was investigated in a separate experiment where the reaction rate was measured at temperatures ranging from 18 to 65 ℃. Arrhenius parameters were determined for pretreatment times of 0 and >70 days for crushed rock masses ranging from 0.2 to 2 g. Fig. 8 indicates that both of rock particles before and after being fully activated shift the Arrhenius plot upwards relative to the homogeneous batch reactor experiment, which results in a larger pre-exponential factor, A, and increased reaction rates. All fitted lines in Fig. 8 were plotted with 95% confidence.

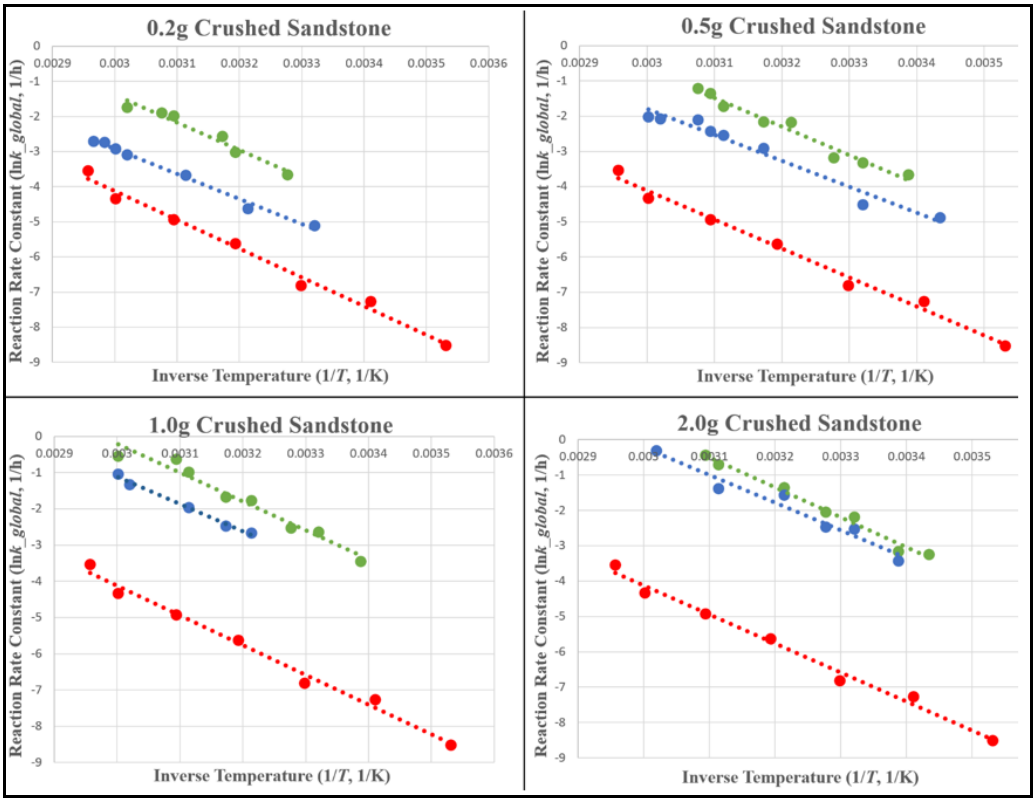

Figure 8: Arrhenius plots comparing the effect of fresh (blue) and fully activated (green) crushed rock particles for a range of crushed rock masses. The homogeneous batch reactor experiment is plotted in red as a reference.

4.3 Derivation of the Global Reaction Rate Expression

Based on the results of the homogeneous and heterogeneous batch reactor experiments, hydrolysis appears to occur in both the fluid and on the surface of silica surfaces. This parallel reaction explains the substantial increase in measured reaction rates. Therefore, the global reaction rate constant, k_{global}, is a function of the overall hydroxide ion concentration, including both the concentration in the fluid and the surface concentration on the rock particles.

The global reaction rate constant as a function of fluid and particle surface hydroxyl concentration is

$$k_{global} = k_{actual} \cdot \left(\left[OH^- \right]_{fluid} + \left[OH^- \right]_{surface} \right) \tag{12}$$

where

$$k_{actual} = \frac{k_{B1} k_{B3}}{k_{B2} + k_{B3}} , \tag{13}$$

$[OH^-]_{fluid}$ is the concentration of hydroxide ions in the fluid, and $[OH^-]_{surface}$ is the surface concentration of hydroxide ions on rock particles. The parameter k_{actual} is equivalent to the first term on the right side of Eqn. (6) and is defined in Eqn. (13). Note that k_{global} and k_{actual} have different units, because the base-catalyzed hydrolysis reaction is not an elementary reaction. Therefore, k_{global} has units of inverse time whereas the units of k_{actual} can be derived based on Eqn. (6).

Based on the results presented in section 4.2, both the effective surface area (*SA*) and the pre-exposure time ($t_{exposure}$) have significant impacts on the global reaction rate constant, k_{global}. Since k_{actual} is independent of these two variables (Eqn. (6)) and $[OH^-]_{fluid}$ is determined by the measured pH, $[OH^-]_{surface}$ is the only term that depends on *SA* and $t_{exposure}$. However, in natural systems, all the rock surfaces can be regarded as already "fully activated" long before tracers are introduced into the geothermal reservoirs. Therefore, the exposure time should be negligible in natural systems and $[OH^-]_{surface}$ could be expressed as

$$\left[OH^- \right]_{surface} = a \cdot SA , \tag{14}$$

where *a* is an unknown constant and *SA* is the effective reactive surface area. In Eqn. (12), the temperature dependency was demonstrated by k_{actual} and the pH dependency was implied by the fluid concentration of hydroxide ions. Combining Eqn. (12) and (14) results in

$$k_{global} = k_{actual} \cdot \left([OH^-]_{fluid} + a \cdot SA \right), \tag{15}$$

where SA is calculated based on the relationship between crushed sandstone masses and surface area. k_{global} and $[OH^-]_{fluid}$ are measured in each experiment. With known Arrhenius parameters for a given surface area (Tbl. 2), the global rate constant, $k_{global-rock}$, can be calculated at a given temperature by

$$k_{global-rock} = A_{rock} \cdot \exp\left(-\frac{E_{a-rock}}{RT}\right) \cdot \tag{16}$$

Based on Eqn. (6) and (7), k_{actual} can be determined using laboratory measurements (Tbl. 1) and the following expression:

$$A_{PhAc} \cdot \exp\left(-\frac{E_{a-PhAc}}{RT}\right) = k_{global-PhAc} = k_{actual} \cdot [OH^-]_{fluid} \cdot \tag{17}$$

Substituting Eqn. (16) and (17) into Eqn. (15) results in an expression relating the Arrhenius parameters as a function of surface area where

$$\frac{A_{rock} \cdot \exp\left(-\frac{E_{a-rock}}{RT}\right) \cdot [OH^-]_{fluid}}{A_{PhAc} \cdot \exp\left(-\frac{E_{a-PhAc}}{RT}\right)} - [OH^-]_{fluid} = [OH^-]_{surface} = a \cdot SA \cdot \tag{18}$$

The unknown constant a in Eqn. (18) can be determined based on a plot of hydroxide ion surface concentration vs. effective surface area. At a fixed temperature, the constant a was calculated for four experiments no. 1 to 4 in Tbl. 2. The average slope of a best-fit line on this plot estimates a (Fig. 9). From 20 to 65 °C, the value of a varies from 2.0×10^{-5} to 3.0×10^{-5} mol/m^2 with an average value of 2.3×10^{-5} mol/m^2. The final expression for the global reaction rate, k_{global}, as a function of temperature, pH, and surface area is

$$k_{global} = \frac{\exp\left(-E_a/RT + \ln A\right)}{[OH^-]_{fluid}} \cdot \left([OH^-]_{fluid} + 2.3 \times 10^{-5} \cdot SA\right) \tag{19}$$

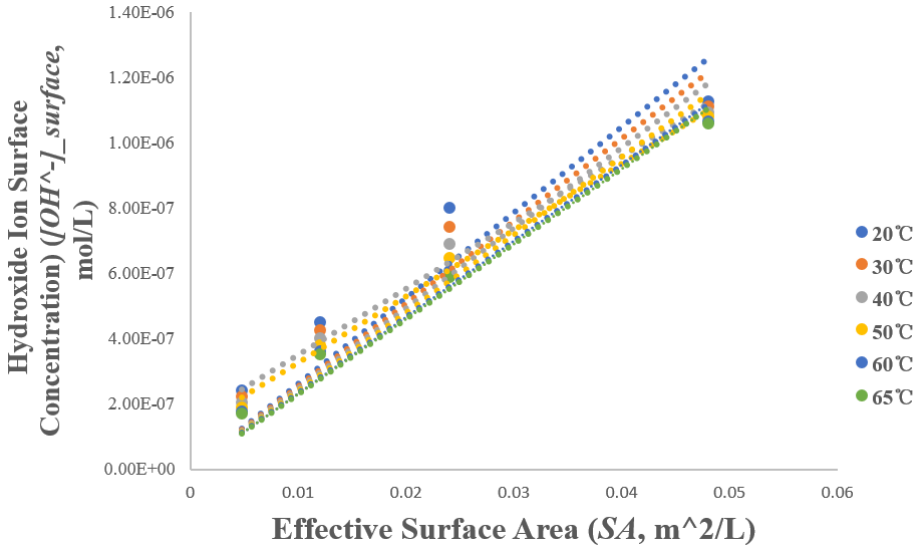

Figure 9: Surface concentration of hydroxide ions is plotted as a function of effective surface area. Slopes of these best-fit lines at various temperatures are the corresponding values of the parameter *a* at each temperature.

5. CONCLUSIONS AND FUTURE WORK

An apparent catalytic effect to the hydrolysis of phenyl acetate was first reported by Hawkins et al. (2017a) where field measurements of phenyl acetate hydrolysis in a sandstone bedding plane resulted in reaction rates more than 7000x greater than reported for laboratory batch experiments (Nottebohm et al., 2012). Laboratory batch reactor experiments discussed here confirmed that the Potsdam Sandstone acts as a catalyst in the hydrolysis of phenyl acetate. A positive correlation was observed between mass of crushed rock and reaction rate constants (Fig. 6). The catalytic effect was quantified in Arrhenius plots and results in an upward shifting of the plots with increasing crushed rock mass (reference to a figure). As a result, the pre-exponential factor was strongly influenced by the mass of rock catalyst. However, the catalyst had less of an effect on the activation energy.

The mechanism responsible for catalysis is not yet known. Potential explanations include microbial activity (e.g., Afrapoli et al., 2009), deposition of metals (e.g., Hemley and Hunt, 1992), or aggregation of hydroxides on the surface of silica particles (e.g., Zhuravlev, 200). Future work will investigate the catalytic mechanism using surface characterization techniques, including Fourier Transform Infrared (FTIR) spectroscopy and Nuclear Magnetic Resonance (NMR).

In the context of identifying thermally degrading tracers for use in the field, the observed catalysis of phenyl acetate hydrolysis by sandstone suggests that hydrolysis reactions may experience heterogeneous reactions too complex for practical application as a tool for monitoring reservoir thermal drawdown. However, if reservoir surface chemistry is adequately known and quantified, their use as a thermally degrading tracer may be appropriate. In fact, the catalytic effect could have some additional benefit if the relationship between fracture surface area and reaction catalyst is adequately quantified in conditions appropriate for geothermal reservoirs.

In addition to surface characterization, future work will include reinterpretation of field tests using thermally degrading tracers. With the measurements presented in this work, the results of field tests presented in Hawkins et al. (2017a) can be reinterpreted using measurements of the Arrhenius parameters as a function of surface area. As a result, temperature estimates from thermally degrading tracer testing will be quantitatively evaluated.

ACKNOWLEDGEMENTS

This study material is based upon work supported in part by the U.S. Department of Energy's Office of Energy Efficiency and Renewable Energy (EERE) under Award Number DE EE0006764, the Cornell Energy Institute, Stanford Geothermal Program, and Stanford University's TomKat Center for Sustainable Energy. Special thanks to Ivan Beentjes, Jared Smith, Xin Zhou, and Arna Pálsdóttir for their assistance in this project.

REFERENCES

Afrapoli, M. S., Crescente, C., Alipour, S., & Torsaeter, O. (2009). The effect of bacterial solution on the wettability index and residual oil saturation in sandstone. Journal of Petroleum Science and Engineering, 69(3), 255-260.

Becker, M. W., Remmen, K., Reimus, P. W., & Tsoflias, G. P. (2013). Investigating well connectivity using ionic tracers. In Thirty-Eighth Workshop on Geothermal Reservoir Engineering, Stanford, California.

Becker, M. W., & Tsoflias, G. P. (2010). Comparing flux-averaged and resident concentration in a fractured bedrock using ground penetrating radar. Water Resources Research, 46(9).

Bjornsson, G., & Steingrimsson, B. (1992). Fifteen years of temperature and pressure monitoring in the Svartsengi high-temperature geothermal field in SW-Iceland. Transactions- Geothermal Resources Council.

Diaz, A. R., Kaya, E., & Zarrouk, S. J. (2016). Reinjection in geothermal fields− A worldwide review update. Renewable and Sustainable Energy Reviews, 53, 105-162.

Hawkins A. J. (2013), Measurement of the spatial distribution of heat exchange in a geothermal analog bedrock site using fiber-optic distributed temperature sensing, M.S. Thesis, California State University, Long Beach.

Hawkins, A. J. (2017). Reactive Tracers for Characterizing Fractured Geothermal Reservoirs, PhD Dissertation, Cornell University.

Hawkins, A.J., M.W. Becker, & G.P. Tsoflias (2017a), Evaluation of inert tracers in a bedrock fracture using ground penetrating radar and thermal sensors, Geothermics, 67, 86-94.

Hawkins, A.J., D.B. Fox, M.W. Becker, & J.W. Tester (2017b), Measurement and simulation of heat exchange in fractured bedrock using inert and thermally degrading tracers, Water Resources Research, 53, doi: 10.1002/2016WR019617.

Hawkins, A. J., M. W. Becker, & J. W. Tester (2018), Inert and adsorbing tracers for field measurement flow-wetted surface area, Water Resources Research, In Review.

Hemley, J. J., & Hunt, J. P. (1992). Hydrothermal ore-forming processes in the light of studies in rock-buffered systems; II, Some general geologic applications. Economic Geology, 87(1), 23-43.

Horne, R. N. (1985). Reservoir engineering aspects of reinjection. Geothermics, 14(2-3), 449-457.

Liu, Q., Ding, J., Mante, F. K., Wunder, S. L., & Baran, G. R. (2002). The role of surface functional groups in calcium phosphate nucleation on titanium foil: a self-assembled monolayer technique. Biomaterials, 23(15), 3103-3111.

Maier, F., Schaffer, M., & Licha, T. (2015). Temperature determination using thermo-sensitive tracers: Experimental validation in an isothermal column heat exchanger. Geothermics, 53, 533-539.

Malate, R. C. M., & O'sullivan, M. J. (1991). Modelling of chemical and thermal changes in well PN-26 Palinpinon geothermal field, Philippines. Geothermics, 20(5-6), 291-318.

Nottebohm, M., Licha, T., & Sauter, M. (2012). Tracer design for tracking thermal fronts in geothermal reservoirs. Geothermics, 43, 37-44.

Robinson, B. A., Tester, J. W., & Brown, L. F. (1988). Reservoir sizing using inert and chemically reacting tracers. SPE Formation Evaluation, 3(01), 227-234.

Schwarzenbach, R. P., & Gschwend, P. M. DM lmboden. 1993. Environmental organic chemistry.

Vides-Ramos, A. (1985), Ahuachapán, El Salvador, field management, Proceedings, in Geothermal Resource Council: International Volume, 397-404

Zhuravlev, L. T. (2000). The surface chemistry of amorphous silica. Zhuravlev model. Colloids and Surfaces A: Physicochemical and Engineering Aspects, 173(1), 1-38.